Contract No:

This document was prepared in conjunction with work accomplished under Contract No. DE-AC09-08SR22470 with the U.S. Department of Energy.

Disclaimer:

WSRC-TR-2006-00321
Revision 0

Decontamination of Zircaloy Spent Fuel Cladding Hulls

Tracy S. Rudisill and John I. Mickalonis

September 2006

Washington Savannah River Company
Aiken, SC 29808

Prepared for the U. S. Department of Energy under Contract DE-AC09-96SR18500 (mod. 68)

Decontamination of Zircaloy Spent Fuel Cladding Hulls

By

Tracy S. Rudisill and John I. Mickalonis

Issued: September 2006

Table of Contents

List of Tables

List of Figures

List of Appendices

Decontamination of Zircaloy Spent Fuel Cladding Hulls

Tracy S. Rudisill and John I. Mickalonis

Washington Savannah River Company
Aiken, SC 29808

Summary

The reprocessing of commercial spent nuclear fuel (SNF) generates a Zircaloy cladding hull waste which requires disposal as a high level waste in the geologic repository. The hulls are primarily contaminated with fission products and actinides from the fuel. During fuel irradiation, these contaminants are deposited in a thin layer of zirconium oxide (ZrO_2) which forms on the cladding surface at the elevated temperatures present in a nuclear reactor. Therefore, if the hulls are treated to remove the ZrO_2 layer, a majority of the contamination will be removed and the hulls could potentially meet acceptance criteria for disposal as a low level waste (LLW). Discard of the hulls as a LLW would result in significant savings due to the high costs associated with geologic disposal.

To assess the feasibility of decontaminating spent fuel cladding hulls, two treatment processes developed for dissolving fuels containing zirconium (Zr) metal or alloys were evaluated. Small-scale dissolution experiments were performed using the ZIRFLEX process which employs a boiling ammonium fluoride (NH_4F)/ammonium nitrate (NH_4NO_3) solution to dissolve Zr or Zircaloy cladding and a hydrofluoric acid (HF) process developed for complete dissolution of Zr-containing fuels. The feasibility experiments were performed using Zircaloy-4 metal coupons which were electrochemically oxidized to produce a thin ZrO_2 layer on the surface. Once the oxide layer was in place, the ease of removing the layer using methods based on the two processes was evaluated.

The ZIRFLEX and HF dissolution processes were both successful in removing a 0.2 μm (thick) oxide layer from Zircaloy-4 coupons. Although the ZIRFLEX process was effective in removing the oxide layer, two potential shortcomings were identified. The formation of ammonium hexafluorozirconate ($(NH_4)_2ZrF_6$) on the metal surface prior to dissolution in the bulk solution could hinder the decontamination process by obstructing the removal of contamination. The thermal decomposition of this material is also undesirable if the cladding hulls are melted for volume reduction or to produce waste forms. Handling and disposal of the corrosive offgas stream and ZrO_2-containing dross must be addressed. The stability of Zr^{4+} in the NHF_4/NH_4NO_3 solution is also a concern. Precipitation of ammonium zirconium fluorides upon cooling of the dissolving solution was observed in the feasibility experiments. Precipitation of the solids was attributed to the high fluoride to Zr ratios used in the experiments. The solubility of Zr^{4+} in NH_4F solutions decreases as the free fluoride concentration increases.

The removal of the ZrO_2 layer from Zircaloy-4 coupons with HF showed a strong dependence on both the concentration and temperature. Very rapid dissolution of the oxide layer and significant amounts of metal was observed in experiments using HF concentrations ≥ 2.5 M. Treatment of the coupons using HF concentrations ≤ 1.0 M was very effective in removing the oxide layer. The most effective conditions resulted in dissolution rates which were less than approximately 2 mg/cm^2-min. With dissolution rates in this range, uniform removal of the oxide layer was obtained and a minimal amount of Zircaloy metal was dissolved. Future HF dissolution studies should focus on the decontamination of actual spent fuel cladding hulls to determine if the treated hulls meet criteria for disposal as a LLW.

Introduction

Background

Light water reactors (LWR) in the United States (US) utilize uranium dioxide fuel (UO_2) clad in a Zircaloy alloy. Older fuels were clad with Zircaloy-2 which provides superior corrosion protection compared to Zr; however, Zircaloy-4 is currently used because the low nickel content reduces hydrogen embrittlement. The composition of the two alloys are shown in Table 1.[1]

Table 1 Zircaloy Alloy Compositions

Element	Zircaloy-2 (wt%)	Zircaloy-4 (wt%)
Tin	1.2-1.7	1.2-1.7
Iron	0.07-0.20	0.18-0.24
Chromium	0.05-0.15	0.07-0.13
Nickel	0.03-0.08	0.007 max
Zirconium	Remainder	Remainder

Spent nuclear fuel from US reactors is currently stored at the site of generation while awaiting final disposition. Since 1968, US nuclear plants have discharged more than 175,000 fuel assemblies containing over 50,000 metric tons of uranium (MTU).[2] If the decision was made to reprocess the SNF, and if the oldest fuel was processed first at a rate which matches the demand for new fuel (~2,500 MTU/yr), the plant would never process fuel cooled for less than 40 years.[3] The long cooling time could facilitate the disposal of the spent fuel cladding hulls as a low level waste (LLW) due to significant decay of the activation and fission products, assuming a majority of the remaining contamination is removed by a decontamination process.

Current LWR fuel reprocessing technology utilizes a chop-leach step to shear fuel rods into short segments (2-5 cm) for subsequent dissolution of the UO_2 in nitric acid. The cladding materials remaining after the dissolution include short lengths of the Zircaloy hulls and varying amounts of fuel hardware. The amount of hardware is dependent upon the type of assembly, degree of disassembly, and sorting prior to the shearing operation. Following the dissolution, the Zircaloy hulls (and associated hardware) are typically rinsed in nitric acid and discarded as waste. In the US, irradiated Zircaloy cladding hulls would be designated a high level waste as defined by the

Nuclear Waste Policy Act.[4] However, if the hulls could be treated to remove a majority of the actinide and fission product contamination, they could potentially meet acceptance criteria for disposal as a LLW. Discard of the hulls as a LLW would not require disposal in the geologic repository and would result in significant cost savings.

During fuel irradiation, radioactive materials including actinides, fission products, and activation products are deposited or produced in Zircaloy cladding. The cladding contamination is produced by a variety of mechanisms which include:[5]

1. Activation of Zircaloy components and impurities (such as U and thorium),
2. Fission recoil deposition,
3. Diffusion of nuclides from the fuel (especially fission products),
4. Occlusion of fission products and actinides into the ZrO_2 during irradiation,
5. Capture of tritium produced in fuel and reactor coolant,
6. Penetration due to corrosion,
7. Physical impaction with UO_2 fuel during shearing,
8. Residual undissolved fuel,
9. Surface contamination resulting from deposition during fuel dissolution.

During irradiation, a thin layer of ZrO_2 is formed on the surface of cladding hulls at the elevated temperatures present in nuclear reactors. The inner surface layer, typically 2-10 μm thick, is a result of reaction with the UO_2 fuel while the outer layer, ranging from 5-50 μm thick, is due to reaction with the reactor coolant.[1,6] Apart from small amounts of residual fuel, fission product and actinide elements are present as deposits formed during fuel dissolution, as nuclides driven into the cladding by fission recoil, and from atomic diffusion into the Zircaloy. Due to the short depths of penetration, both fission products and actinide elements are predominately located in the ZrO_2 layer on the surface of the cladding.[5] Therefore, if the ZrO_2 layer can be removed from the cladding hulls, the majority of the fission product and actinide contamination will also be removed.

Cladding Decontamination

In an assessment of decontamination technology for spent fuel cladding hulls, Witt [5] identified two reprocessing flowsheets with the potential for chemically decontaminating the hulls. The first, the ZIRFLEX process, employs a boiling aqueous solution of NH_4F and NH_4NO_3 to dissolve Zr or a Zircaloy alloy (equation 1).

$$Zr_{(s)} + 6NH_4F + 0.5NH_4NO_3 \rightarrow (NH_4)_2 ZrF_6 + 5NH_{3(g)} + 1.5H_2O \qquad (1)$$

The process was developed at the Department of Energy's (DOE's) Hanford site for the reprocessing of slightly enriched power reactor fuels. Initially, the Zircaloy cladding was chemically removed using a boiling 5.5 M NH_4F/0.5 M NH_4NO_3 solution at a fluoride/Zr mole ratio of 7. Average unoxidized Zircaloy dissolution rates were from 10-15 mils/h. The time required for decladding a 30-40 mil unoxidized fuel element was 3-4 h; however, the removal of oxidized Zircaloy cladding could require up to 12 h. During cladding dissolution, ammonia (NH_3) must be removed from the dissolvent to prevent a decrease in the dissolution rate and a

lowering of the Zr^{4+} stability. The solubility of the $(NH_4)_2ZrF_6$ complex formed during the ZIRFLEX dissolution depends on the free fluoride concentration, ammonium ion concentration, and temperature. To achieve optimum dissolution conditions, NH_3 formed during the reaction is removed to provide a slightly acidic solution (pH 6-7). Once the cladding dissolves, the waste solution is removed from the dissolver and boiling 4 M nitric acid is used to dissolve the UO_2 fuel. Aluminum nitrate is added to the dissolver to inhibit corrosion.[7]

The second process proposed for hull decontamination is based on reprocessing flowsheets for Zircaloy-based reactor fuels developed at DOE's Idaho Chemical Processing Plant. These processes utilized aqueous solutions of HF to dissolve both fuel and cladding. The flowsheets were generally characterized as concentrated or dilute based on the HF concentration. The concentrated flowsheets took advantage of the very high solubility of Zr in nominally 10 M HF and the high dissolution rates characteristic of the acidity. However, the concentrated flowsheets had the disadvantage of not dissolving the U in fuels containing greater than about 1% U unless relatively powerful oxidants were added to facilitate the UO_2 dissolution. The addition of an oxidant increased corrosion problems associated with the process. The dilute flowsheets used nominally 5 M HF for the batch dissolution of both Zr and U from fuels containing 2% or greater U. Dissolution was readily initiated and sustained at 30 °C (or higher if desired) for either flowsheet. Typical dissolving solution compositions for both the concentrated and dilute flowsheets are summarized in Table 2.[8]

Table 2 Solution Compositions for HF Dissolution Flowsheets

Component	Concentrated Flowsheet Composition (M)	Dilute Flowsheet Composition (M)
H^+	10.0	4.84
F^-	10.0	4.81
H_2O_2	0.01	
NO_3^-		0.027(1)
B	0.093(2)	0.093(2)

(1) Nitric acid was used for the oxidation of tin.
(2) Boron was used as a nuclear safety poison.

Experimental Objectives

Both the ZIRFLEX and HF dissolution processes can remove the ZrO_2 layer from spent fuel cladding hulls. To evaluate the practicality of using a modification to one of these processes in a large-scale spent fuel reprocessing facility to decontaminate cladding hulls, small-scale feasibility experiments were performed. The feasibility experiments were performed using Zircaloy-4 metal coupons. Prior to the dissolution studies, a ZrO_2 layer was grown on the surface of the metal using an electrochemical oxidation process. Once the oxide layer was in place, the ease of removing the layer using methods based on the ZIRFLEX and HF dissolution processes was evaluated.

Experimental

Growth of Zircaloy-4 Oxide Layer

To evaluate the feasibility of decontaminating spent fuel cladding hulls using a modification to the ZIRFLEX and HF dissolution processes, Zircaloy-4 samples were obtained as test materials. The samples were procured from Metal Samples Co., Munsford, AL as disks with a 0.75-in (1.91-cm) diameter and a 0.125-in (0.32-cm) thickness. A certified material test report was obtained to verify the sample composition. Preparation of the Zircaloy-4 samples for the dissolution tests included the growth of a oxide layer on the samples using an electrochemical technique. With electrochemical oxidation, a thin (<1 μm) uniform oxide layer was grown under low-temperature, high-voltage conditions in a chemical solution.

To grow the oxide layer, an electrical wire was attached to one side of the sample with a silver-based epoxy. The sample was then cast into an epoxy mount. The sample surface was prepared using a 600 grit silicon carbide paper without additional processing. Surfaces were cleaned with ethyl alcohol prior to oxidation. Electrochemical oxidation was performed by applying a high anodic voltage across the Zircaloy-4 interface for a given time period at room temperature by immersing the sample into a 0.1 M sodium hydroxide solution contained in a glass beaker. A graphite rod was used as a counter electrode for current conduction. Oxidation started immediately after sample immersion and stopped when the current dropped to zero. An Ametek PAR galvanostat/potentiostat Model 273A was used for applying the voltage. The experimental equipment is shown in Figure 1.

Oxide Layer Thickness Measurement

An attempt to measure the thickness of the ZrO_2 layer formed during the electrochemical oxidation process was initially performed using a scanning electron microscope; however, the layer thickness was too thin to accurately measure. In the absence of an instrumental technique, the color of the oxidized coupon was used to estimate the thickness of the oxide layer. A correlation of ZrO_2 layer thickness with color (Figure 2) was obtained from the Chalk River Laboratories, Chalk River, Ontario, Canada.[9] When the oxidation current dropped to zero, the surface of the Zircaloy-4 coupon was light green in color which corresponds to an oxide layer thickness of nominally 0.20 μm. A photograph of oxidized and unoxidized coupons is shown in Figure 3 for comparison.

Oxide Removal Tests

ZIRFLEX Dissolution Process

The ZIRFLEX dissolution tests were performed in a glass vessel fabricated from a 250 mL three-neck, round-bottom flask. The dissolving solution was heated and stirred using a heating mantle equipped with a magnetic stirrer. The temperature of the dissolving solution was monitored using a type J thermocouple. A glass thermowell was used to isolate the thermocouple from the dissolving solution. A water-cooled condenser was attached to the flask to reduce the evaporation of solution during heating. A porous glass basket attached to the

center stopper was used to hold the Zircaloy coupon and to allow inspection during a dissolution. A compression fitting used as a penetration in the stopper provided the capability to adjust the depth of the basket in the vessel. A separate penetration in the vessel wall was provided so air could be used to purge NH_3 from the dissolving flask. Photographs of the dissolution vessel and glass basket are shown in Figure 4.

The ZIRFLEX dissolution experiments were each performed using a 150 mL aliquot of solution. The solution was heated to the desired temperature before the Zircaloy coupon was placed in the vessel. A summary of the experimental conditions for each dissolution is provided in Table 3.

Table 3 Experimental Condition for ZIRFLEX Dissolutions

Exp't No.	NH_4F (M)	NH_4NO_3 (M)	Temp. (°C)	Air Purge (SCFH)
ZF-1	5.5	0.5	104	N/A
ZF-2	5.5	0.5	80	N/A
ZF-3	5.5	0.5	102	N/A
ZF-4	5.5	0.5	102	N/A
ZF-5	5.5	0.5	80	N/A
ZF-6	2.75	0.25	101	N/A
ZF-7	5.5	0.5	102	4

Since the amount of ZrO_2 and Zircaloy-4 metal dissolved during each experiment was relatively small, multiple experiments were performed using the same solution. Experiments ZF-1, ZF-2, and ZF-3 were performed with a single 150 mL aliquot of solution as were experiments ZF-4 and ZF-5. The dissolution experiments were either performed at 80 °C or at the boiling point of the solution. The slightly different temperature readings given in Table 3 for the boiling point reflect the variability in the thermocouple reading. In experiment ZF-7, a 4 SCFH (110 standard L/h) air stream was used to purge NH_3 from the vessel. Once the temperature of the dissolving solution stabilized at the target value, the Zircaloy coupon was placed in the glass basket and immersed in the solution. The basket was periodically removed from the vessel to inspect the coupon. Prior to inspection, the coupon was rinsed with deionized water to remove any of the dissolvent. Observations concerning the color and appearance of the coupon were noted during the inspections. The dissolution was terminated when color due to the oxide layer (see Figure 2) was no longer observed on the surface of the coupon. The cumulative dissolution time was measured using a stop watch. In order to obtain an estimate of the dissolution rate of the oxidized coupons, the mass and surface area (i.e., diameter and thickness) of the coupons were measured before and after each experiment. The dissolution rates were then calculated as the change in the mass to surface area ratio with respect to time.

HF Dissolution Process

Due to the corrosiveness of HF (especially to glass), a 250 mL Teflon® beaker was used for the primary containment vessel for the HF dissolutions. The beaker was heated and stirred using a hot plate equipped with a magnetic stirrer. A thermocouple probe connected to the hot plate was used for temperature control. To prevent excessive evaporation of HF, a water-cooled, glass top

was used to partially seal the beaker. The glass to beaker seal was improved by using an o-ring and wrapping the insert which extended into the beaker with Teflon® tape. A gas tight seal was not desired. Two penetrations were provided in the glass top to accommodate the hot plate thermocouple and a Teflon® rod which supported a porous Teflon® basket. The basket was used to hold the Zircaloy coupon during dissolution. The basket provided the capability to easily remove the coupon for inspection during a dissolution. The compression fittings used for both penetrations provided the capability to adjust the depth of the thermocouple and basket in the beaker. Photographs of the dissolution vessel and Teflon® basket are shown in Figure 5.

To perform an HF dissolution experiment, 150 mL of solution of the desired concentration were transferred to the Teflon® beaker. The solution was then heated to the target temperature before the Zircaloy coupon was placed in the vessel. Since the amount of Zr dissolved during each experiment was relatively small, the same solution was used to perform all dissolutions at the same HF concentration. A summary of the experimental conditions for each dissolution is provided in Table 4.

Table 4 Experimental Conditions for HF Dissolutions

Exp't No.	HF (M)	Temp. (°C)
HF-1	5.0	60
HF-2	5.0	40
HF-3	2.5	60
HF-4	2.5	40
HF-5	1.0	60
HF-6	1.0	40
HF-7	1.0	40
HF-8	0.5	60
HF-9	0.5	40

After the Zircaloy coupon was placed in the Teflon® basket and immersed in the solution, the basket was periodically removed from the beaker to inspect the coupon. Prior to inspection, the coupon was rinsed with deionized water to remove any HF. Observations concerning the color and appearance of the coupon were noted during the inspections. The dissolution was terminated when color due to the oxide layer (see Figure 2) was no longer observed on the surface of the coupon. The cumulative dissolution time was measured using a stop watch. In order to obtain an estimate of the dissolution rate of the oxidized coupons, the mass and surface area of the coupons were measured before and after each experiment. The dissolution rates were then calculated as the change in the mass to surface area ratio with respect to time.

Results and Discussion

ZIRFLEX Dissolutions

The dissolution time and general observations for each ZIRFLEX experiment are summarized in Table 5. The dissolution temperature for each experiment is also included in the table for reference.

Table 5 Observations from ZIRFLEX Dissolution Experiments

Exp't No.	Time (min)	Temp. (°C)	Observations
ZF-1	2	104	Vigorous reaction observed; oxide layer removed; black residue visible on coupon surface.
ZF-2	8	80	Oxide layer still visible after 4 min; oxide removed after 8 min; black residue removed from surface with cloth.
ZF-3	6	102	Oxide layer still visible after 2 min; no oxide visible after 6 min; black residue coated surface of coupon.
ZF-4	12	102	Vigorous reaction; black residue formed on surface dissolves in solution; no oxide visible on surface following experiment.
ZF-5	60	80	Removal of oxide much slower; lower temperature minimizes amount of black residue; no oxide visible on coupon.
ZF-6(1)	60	101	Oxide layer was removed; black residue formed on the surface was easily removed with cloth wipe.
ZF-7(2)	18	102	Oxide layer not observed after 3 min; black residue present on surface; purge had no impact on the oxide removal.

(1) 2.25 M NH_4F/0.25 M NH_4NO_3 used for dissolving solution.
(2) 4 SCFH air purge used during dissolution.

As noted in Table 5, the ZrO_2 layer was removed from the Zircaloy coupons in each of the dissolution experiments. When traditional ZIRFLEX processing conditions (i.e., boiling 5.5 M NH_4F/0.5 M NH_4NO_3) were used, the oxide layer was removed in 2-6 min. Reductions in either temperature or the reagent concentrations resulted in longer dissolution times. In order to quantify the rate at which the oxidized coupons dissolved, effective dissolution rates were calculated for experiments ZF-4 through ZF-7. The rate was calculated from the change of the mass to surface area ratio at the beginning and end of the dissolution. The calculation of the rates is summarized in Appendix A. A summary of the conditions and measured rates for the experiments are given in Table 6.

Table 6 Effective ZIRFLEX Dissolution Rates

Exp't No.	NH_4F (M)	NH_4NO_3 (M)	Temp. (°C)	Effective Rate (mg/cm^2-min)
ZF-4	5.5	0.5	102	9
ZF-5	5.5	0.5	80	2
ZF-6	2.75	0.25	101	3
ZF-7	5.5	0.5	102	10

The dissolution rates measured using boiling 5.5 M NH_4F/0.5 M NH_4NO_3 are generally consistent with dissolution rates measured during the development of the ZIRFLEX process using similar free fluoride concentrations under laboratory conditions.[7] The dissolution rate is also reported to increase regularly with increasing NH_4F concentration up to approximately 6 M. Above this concentration, the formation of a protective layer of $(NH_4)_2ZrF_6$ on the surface of the metal can actually reduce the rate of dissolution.[10]

To identify the black residue which formed on (and subsequently dissolved from) the surface of the Zircaloy coupons during the experiments (Figure 6), a small sample of the solids from a coupon was dried and analyzed by x-ray diffraction (XRD). The spectrum from the analysis (Figure 7) showed the presence of silver (Ag), tin (Sn), ZrO_2, and $(NH_4)_2ZrF_6$,. A Ag-based epoxy was used to attach an electrical wire to the coupon during the oxidation process and Sn is present at 1.2-1.7 wt% in the Zircaloy-4 alloy; therefore, the presence of these elements in the residue is not unexpected. The ZrO_2 was either incompletely removed from the coupon surface or formed during the dissolution process. The $(NH_4)_2ZrF_6$ is a product of the dissolution of Zr metal using an NH_4F/NH_4NO_3 solution (equation 1).

$$Zr_{(s)} + 6NH_4F + 0.5NH_4NO_3 \rightarrow (NH_4)_2 ZrF_6 + 5NH_{3(g)} + 1.5H_2O \quad (1)$$

The generation of a residue on the surface of spent fuel cladding hulls during decontamination is undesirable. The residue could hinder the decontamination process by obstructing the removal of contamination from the surface of the hulls. The presence of $(NH_4)_2ZrF_6$ in the residue could also interfere with downstream processes if the cladding hulls are melted for either volume reduction or to produce waste forms from other materials, such as recovered technetium and undissolved solids from the dissolver. Thermal decomposition of the $(NH_4)_2ZrF_6$ when the cladding hulls are melted would produce an extremely corrosive offgas stream and a ZrO_2-containing dross. These secondary waste streams would require subsequent treatment for disposal. Removal of the residue from the cladding hulls by vigorously washing with dilute nitric acid may remove a majority of the residue; however, complete removal from all surfaces is doubtful. No attempt to wash the residue from the Zircaloy coupons was performed as part of this study; although, a majority of the residue was removed from some of the coupons by wiping with a cloth.

Another undesirable result identified during the ZIRFLEX experiments was the precipitation of solids from the dissolving solution upon cooling. The solids which precipitated from the solution used to perform experiments ZF-4 and ZF-5 and from the solution used to perform

experiment ZF-7 were recovered by filtration, dried, and subsequently analyzed by XRD. The XRD spectra (Figures 8 and 9) show predominately ammonium zirconium fluorides. From the small amount of Zr dissolved in these solutions, one would normally expect the zirconium fluorides to remain in solution. However, solubility data for Zr in NH_4F solutions (Table 7) show that the solubility of Zr^{4+} decreases as the free fluoride concentration increases.[10]

Table 7 Solubility of Zr in NH_4F at 22 °C

Zr^{4+} (M)	Total Fluoride (M)	NH_4^+ (M)	NO_3^- (M)	pH	Free Fluoride (M)
1.19	7.0	2.22		4.1	0.0
1.00	6.2	2.14		5.3	0.2
0.58	4.4	1.76		5.7	0.9
0.41	3.6	1.70		7.0	1.1
0.37	3.3	1.76		6.0	1.1
0.16	2.5	2.01		6.4	1.6
0.13	2.8	2.14		6.7	2.0
0.037	(4.0)	(4.0)			4.0
0.025	(6.0)	(6.0)			6.0
0.53	3.8	1.88	(0.5)	5.9	0.6
0.23	2.6	2.00	(0.5)	6.1	1.2
0.10	2.3	2.51	(0.5)	6.4	1.7
0.91	5.8	2.85	(1.0)	4.6	0.4
0.89	5.8	2.87	(1.0)	5.0	0.4
0.24	2.2	2.30	(1.0)	5.9	0.7
0.068	2.3	3.16	(1.0)	6.3	1.9

(1) Free fluoride defined as total fluoride (M) - $6xZr^{4+}$ (M).
(2) Values in parentheses deduced from amounts of reagents employed.

The precipitation of the ammonium zirconium fluorides when the solutions cooled was probably due to the extremely high fluoride to Zr ratios in the solutions (31, ZF-4/ZF-5 and 21, ZF-7) and the resulting high concentrations of free fluoride which reduced the solubility of these species. The fact that the primary ammonium zirconium fluoride identified in the solids from experiment ZF-7 (which had the lower Zr to fluoride ratio of the two dissolving solutions) was the heptafluorozirconate ($(NH_4)_3ZrF_7$) is consistent with this argument; the $(NH_4)_3ZrF_7$ is reported to have a lower solubility in NH_4F solutions than the $(NH_4)_2ZrF_6$.[10]

HF Dissolutions

The time and general observations for each HF dissolution experiment are summarized in Table 8. The dissolution temperature and HF concentration for each experiment are also included for reference.

Table 8 Observation from HF Dissolution Experiments

Exp't No.	Time (min)	Temp (°C)	HF (M)	Observations
HF-1	0.33	60	5.0	Rapid dissolution of coupon observed; material spalled away from surface; pitting observed; oxide layer removed.
HF-2	0.5	40	5.0	Dissolution less rapid than at 60 °C; material spalled away from surface and pitting observed; oxide layer removed.
HF-3	1.33	60	2.5	Rapid dissolution with spalling of material from surface observed; oxide layer removed.
HF-4	4	40	2.5	Oxide layer removed; changes in surface color (green to yellow) observed; spalling of material observed after oxide removed.
HF-5	6	60	1.0	Change in surface color during oxide layer removal; material begin to spall from surface after oxide layer removed.
HF-6	6	40	1.0	Change in surface color observed as oxide layer removed; Zircaloy coupon appeared silver, but turned pink when dry.
HF-7	14	40	1.0	Change in surface color observed during dissolution; coupon surface appeared polished upon removal from solution.
HF-8	6	60	0.5	Oxide layer appeared to be gone when removed from solution; after drying coupon had some black discoloration.
HF-9	18	40	0.5	Changes in surface color observed; surface appeared clean, but black coloration formed; crevices on surface.

The ZrO_2 layer was removed from the surface of the Zircaloy coupons in each experiment as noted in the observations summarized in Table 8. Very rapid dissolution of material was observed in the experiments performed using concentrations of HF $\geq$ 2.5 M. Significant amounts of metal were dissolved in very short periods of time. During the dissolutions, the spalling of material from the surface of the coupons was also observed. The surface of the coupons following the dissolutions were generally pitted and very rough (Figure 10). Dissolution of the coupons using concentrations of HF $\leq$ 1.0 M was generally effective in removing the oxide layer without dissolving significant quantities of metal. In order to quantify the rate at which the oxidized coupons dissolved, effective dissolution rates were calculated for each experiment. The rate was calculated from the change of the mass to surface area ratio at the beginning and end of the dissolution. The calculation of the rates is summarized in Appendix B. A summary of the conditions and measured dissolution rates for each experiment are given in Table 9.

Table 9 Effective HF Dissolution Rates

Exp't No.	HF (M)	Temp. (°C)	Effective Rate (mg/cm^2-min)
HF-1	5.0	60	380
HF-2	5.0	40	170
HF-3	2.5	60	100
HF-4	2.5	40	12
HF-5	1.0	60	7.4
HF-6	1.0	40	1.6
HF-7	1.0	40	0.48
HF-8	0.5	60	1.3
HF-9	0.5	40	0.75

The effective rates measured for the HF dissolutions show a strong dependence on both concentration and temperature. The rates are plotted as a function of HF concentration and temperature in Figure 11. The most effective conditions for the removal of the oxide layer from the Zircaloy coupons resulted in dissolution rates which were less than approximately 2 mg/cm^2-min. Dissolution rates in this range resulted in the uniform removal of the oxide layer and minimized the amount of metal dissolved. The uniform removal of the oxide layer obtained in experiment HF-6 is illustrated in Figure 12. The figure compares the appearance of the Zircaloy coupon before and after dissolution in 1.0 M HF at 40 °C for 6 min. Initially the oxidized surface of the coupon was light green in color, corresponding to a nominal oxide layer thickness of 0.2 μm. The coupon was then placed in the HF solution for 6 min. When the coupon was removed, the surface appeared similar to the surface of an unoxidized coupon (Figure 3); however, when the coupon dried, the surface was pink corresponding to an nominal oxide layer thickness of 0.02 μm, suggesting the coupon did not remain in the HF solution long enough for complete removal of the ZrO_2 layer.

Adjusting the effective dissolution rate of oxidized Zircaloy to a value less than 2 mg/cm^2-min can be accomplished by changing combinations of the HF concentration and temperature. Based on the data in Table 9, HF concentrations greater than about 1 M would result in rates significantly greater, resulting in dissolution of more metal than desired. Temperatures greater than 60 °C were not investigated to limit the corrosiveness of the HF; although, higher temperatures may be appropriate for low concentrations (≤ 1 M). The oxide layer can also be removed from Zircaloy by extending the time to compensate for a lower dissolution rate. Subsequent investigation of the ability of HF solutions to decontaminate actual spent fuel cladding hulls should address optimization of the concentration, temperature, and dissolution time to produce a hull which meets the criteria for disposal as a LLW. Minimization of the amount of HF used to decontaminate the hulls should also be a consideration due to the cost of final disposal.

Conclusions

Small-scale experiments were completed to evaluate the feasibility of using the ZIRFLEX and HF dissolution processes to decontaminate cladding hulls from the reprocessing of SNF. The feasibility studies were completed by evaluating the capability of each process to remove an electrochemically grown 0.2 μm (thick) ZrO_2 layer from Zircaloy-4 coupons.

Although the ZIRFLEX process was effective in removing the oxide layer, two potential short comings were identified. During the dissolution of Zr metal in NH_4F solutions, $(NH_4)_2ZrF_6$ forms on the metal surface prior to dissolution in the bulk solution. The presence of a residue on the surface of the cladding hulls could hinder the decontamination process by obstructing the removal of contamination. The fluoride-containing residue is also detrimental if the cladding hulls are melted for either volume reduction or to produce waste forms. The thermal decomposition of $(NH_4)_2ZrF_6$ when cladding hulls are melted would produce an extremely corrosive offgas stream and a ZrO_2-containing dross. Both waste streams would require subsequent treatment for disposal. Another undesirable result identified during the ZIRFLEX experiments was the precipitation of solids from the dissolving solution upon cooling. X-ray diffraction analyses indicated the solids were predominately ammonium zirconium fluorides. Precipitation of the solids was attributed to the extremely high fluoride to Zr ratios used in the experiments. The solubility of Zr in NH_4F solutions decreases as the free fluoride concentration increases.

The removal of the ZrO_2 layer from Zircaloy-4 coupons with HF showed a strong dependence on both the concentration and temperature. Very rapid dissolution of the oxide and metal was observed in experiments performed using HF concentrations $\geq$ 2.5 M. The oxide layer was removed and significant amounts of metal were dissolved in a very short amount of time. Treatment of the coupons using HF concentrations $\leq$ 1.0 M was very effective in removing the oxide layer. The most effective conditions resulted in dissolution rates which were less than approximately 2 mg/cm^2-min. With dissolution rates in this range, uniform removal of the oxide layer was obtained and a minimal amount of Zircaloy metal was dissolved.

Recommendations

Continued development of a decontamination process for spent fuel cladding hulls should focus on the use of HF for removal of the oxide layer and embedded contamination. Future studies performed with actual spent fuel cladding hulls are required to determine if the decontaminated hulls meet criteria for disposal as a LLW. Additional areas of investigation should include process optimization studies focused on the minimization of the amount of HF used in the process and the amount of Zr dissolved during decontamination. These activities are required for waste minimization. The disposal path for the decontamination solution used in a large-scale spent fuel treatment facility should also be identified.

References

1. Technical Committee Meeting Report, *Management of Cladding Hulls and Fuel Hardware*, Technical Report Series No. 258, International Atomic Energy Agency, Vienna, Austria (1985).

2. "Spent Fuel Discharges," *Nuclear News*, p. 68 (December 2004).

3. G. D. DelCul, B. B. Spencer, and E. D. Collins, "*Development of an Advanced Hybrid Pyro/Aqueous Process for Spent Fuel,"* 29th Actinide Separations Conference, Nashville, TN Oak Ridge National Laboratory, Oak Ridge, TN (May 2005).

4. The Nuclear Waste Policy Act of 1982 as Amended (March 2004).

5. D. C. Witt, *Decontamination and Disposal of Zircaloy Spent Fuel Cladding Hulls*, Report WSRC-TR-2005-00350, Westinghouse Savannah River Company, Aiken, SC (September 2005).

6. R. G. Nelson and B. Griggs, *Chop-Leach Fuel Bundle Residues: Densification by Melting*, Report BNWL-SA-5704, Battelle Pacific Northwest Labs, Richland, WA (1976).

7. P. W. Smith, *The ZIRFLEX Process Terminal Development Report*, Report HW-65979, Hanford Atomic Products Operation, Richland, WA (September 1960).

8. C. E. Stevenson, E. A. Mason, and A.T. Gresky, eds., *Progress in Nuclear Energy, Series III, Process Chemistry*, Vol. 4, Pergamon Press, New York, NY, pp. 175-177 (1970).

9. Personal communication from G. McRae, Atomic Energy of Canada, Ltd., Chalk River Laboratories, Chalk River, Ontario, Canada, December 19, 2005.

10. J. L. Swanson, *The Selective Dissolution of Zirconium or Zircaloy Cladding by the Zirflex Process*, Proceedings of the Second United Nations International Conference on the Peaceful Uses of Atomic Energy, Volume 17, Processing Irradiated Fuels and Radioactive Materials, United Nations, Geneva, Switzerland (1958).

Figure 1 Electrochemical Oxidation Equipment

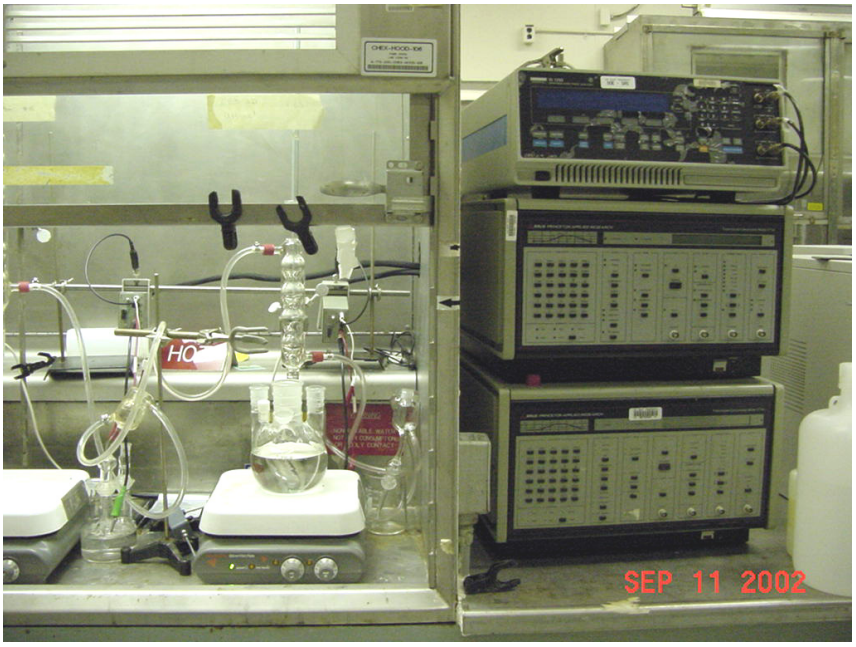

Figure 2 Correlation of ZrO_2 Layer Thickness with Color

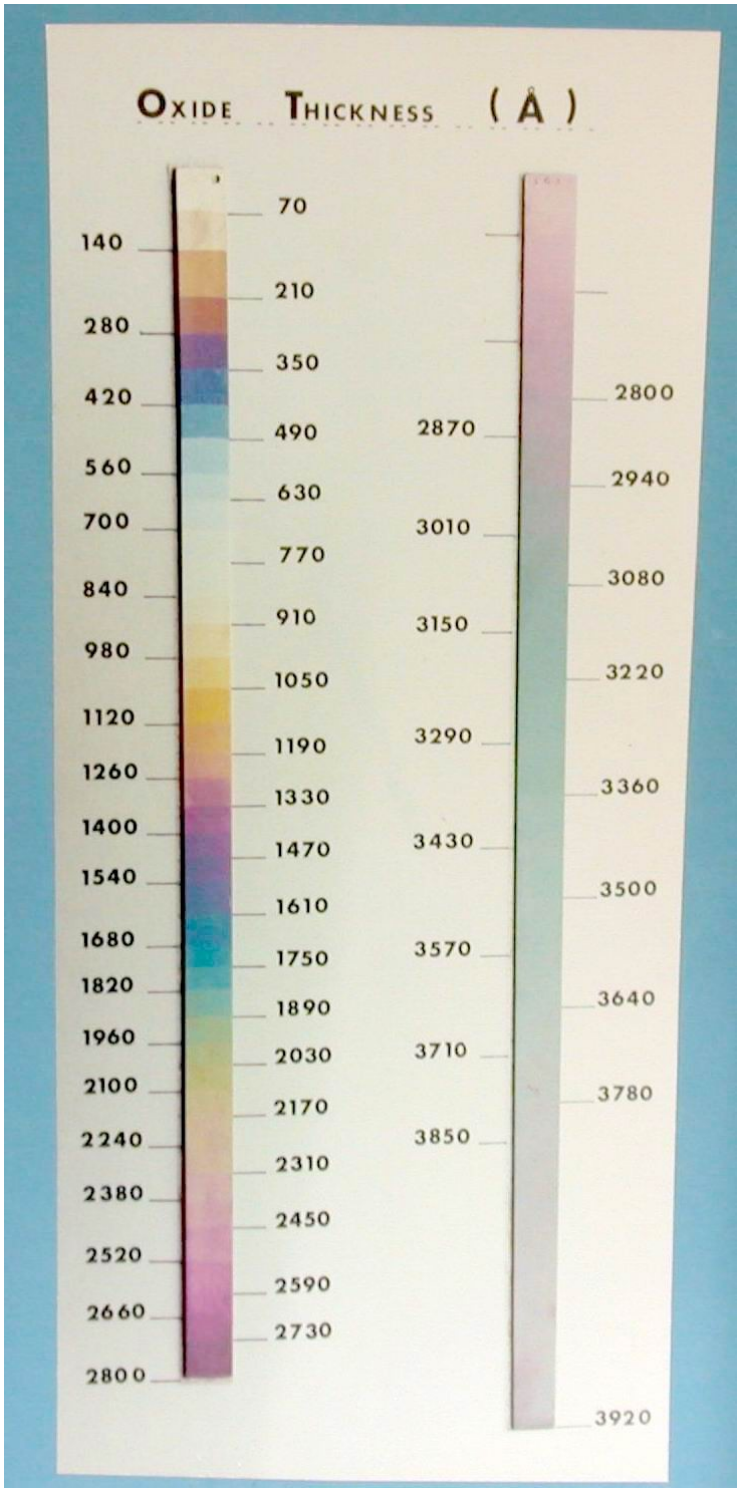

[9] Courtesy of Chalk River Laboratories, Chalk River, Ontario, Canada

Figure 3 Comparison of Oxidized and Unoxidized Zircaloy-4 Coupons

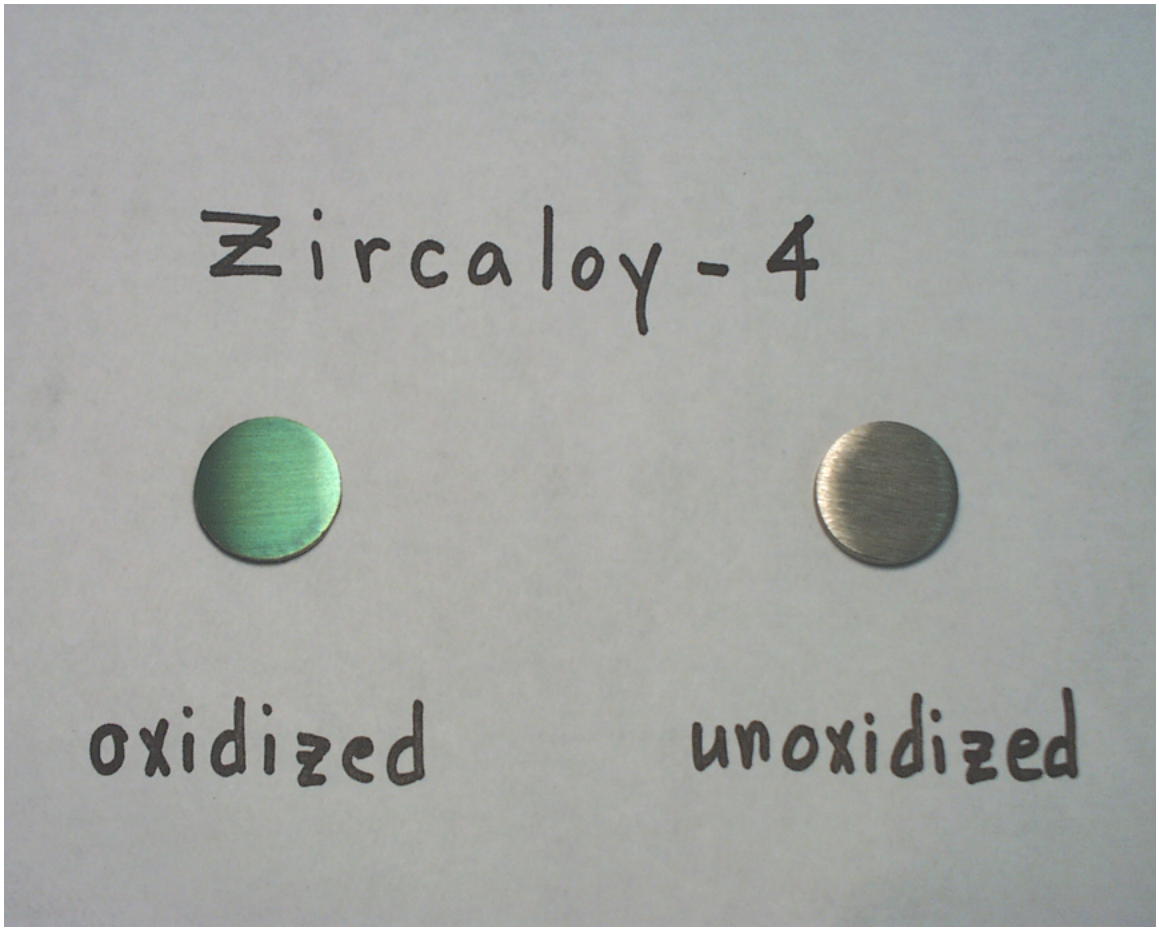

Figure 4 ZIRFLEX Dissolution Equipment

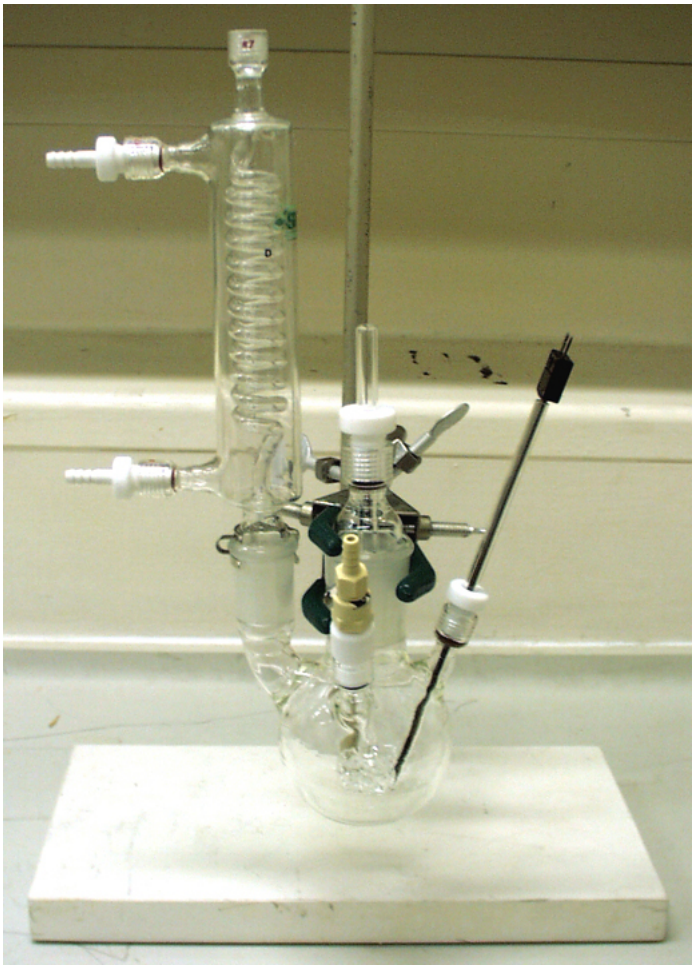

Dissolution Vessel

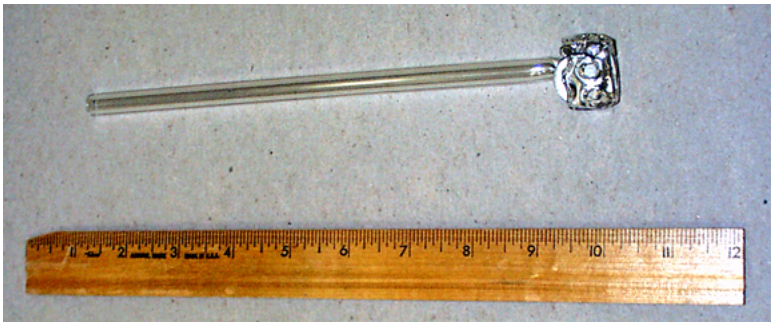

Glass Basket

Figure 5 HF Dissolution Equipment

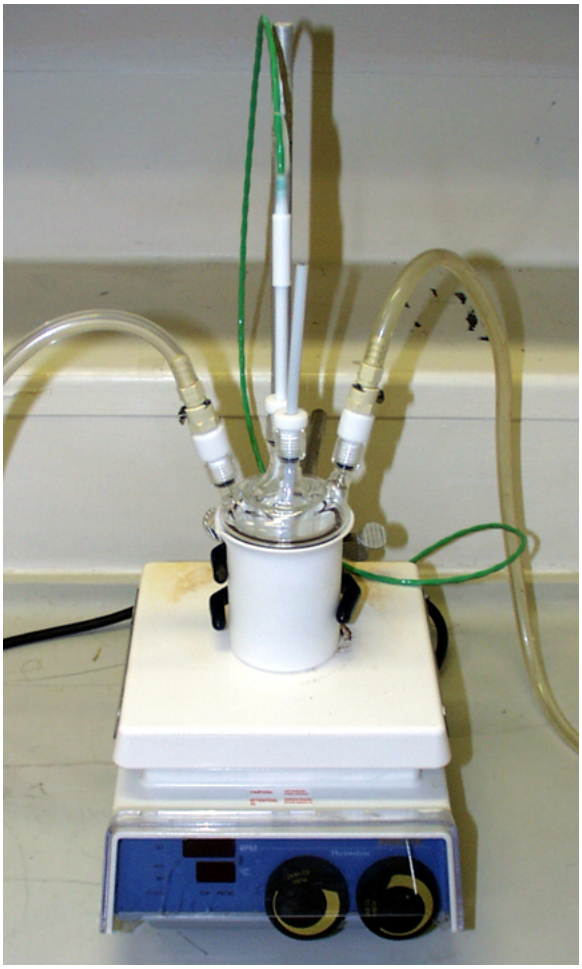

Dissolution Vessel

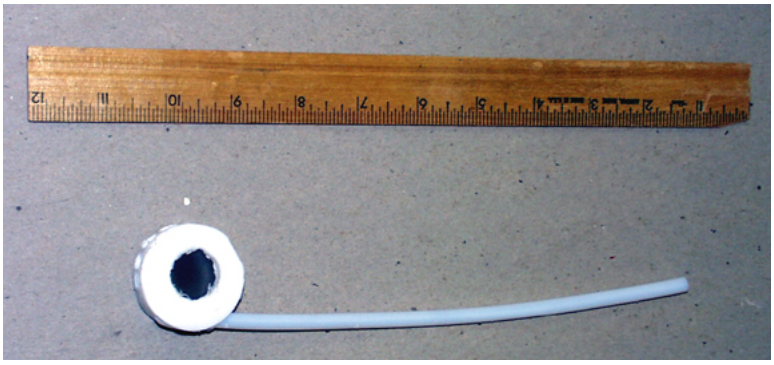

Teflon® Basket

Figure 6 Residue Formed on Zircaloy Coupon Surface During ZIRFLEX Dissolution

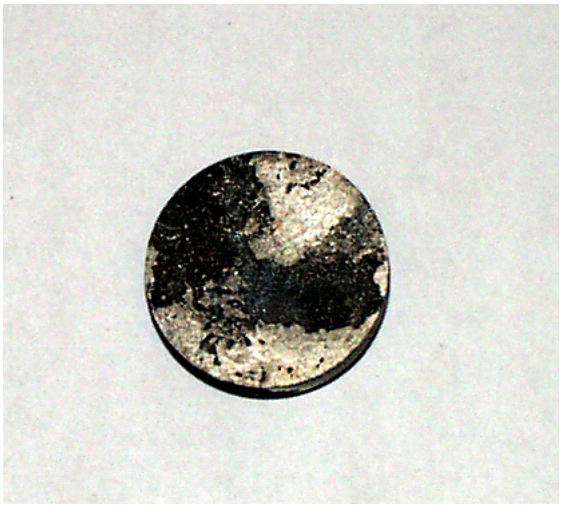

Figure 7 XRD Spectrum of ZIRFLEX Dissolving Residue

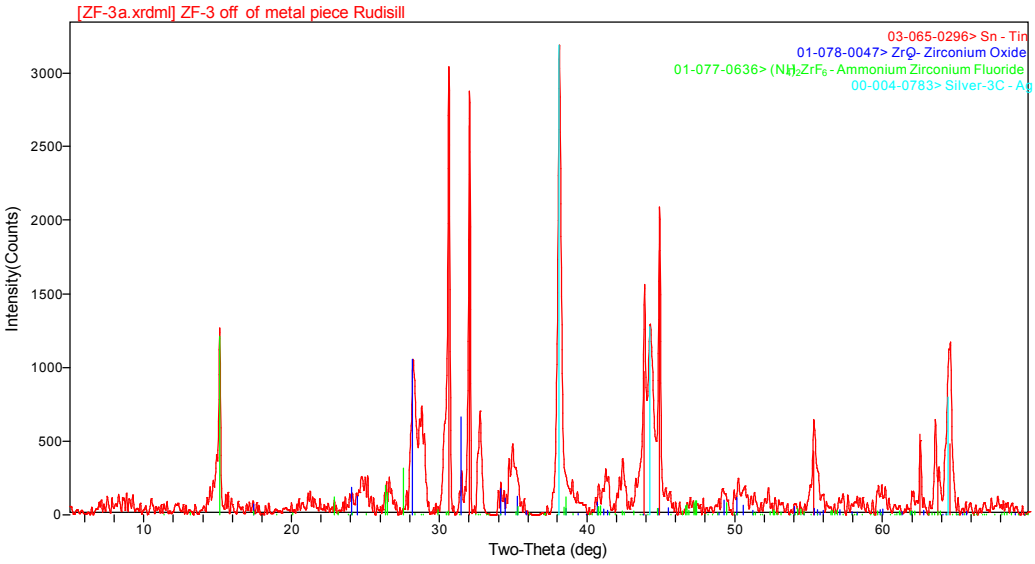

Figure 8 XRD Spectrum of Solids Precipitated from ZF-4 and ZF-5 Dissolving Solution

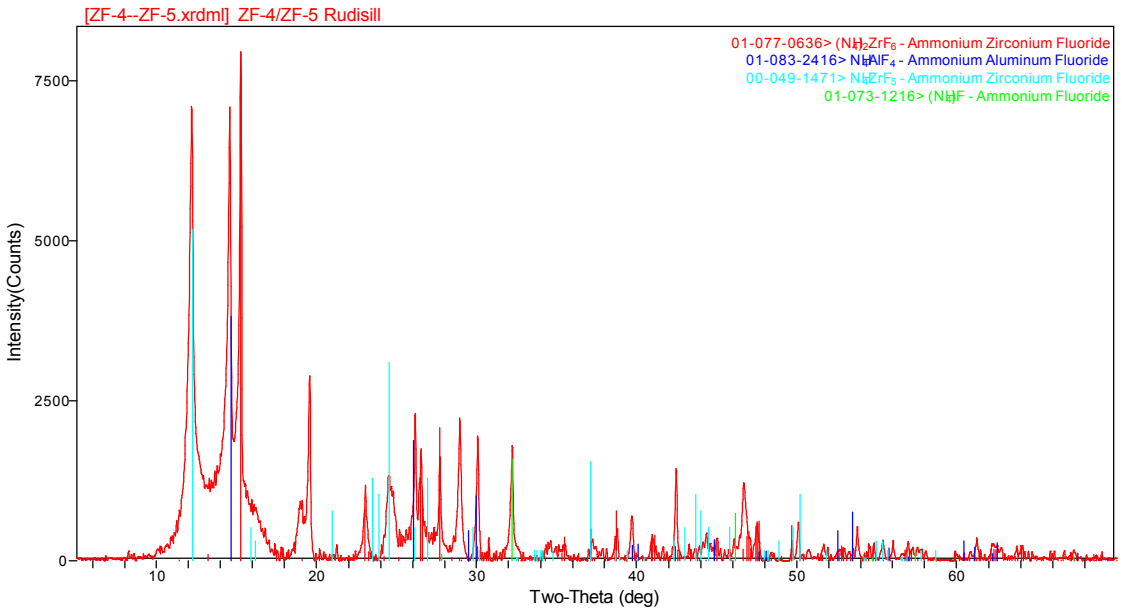

Figure 9 XRD Spectrum of Solids Precipitated from ZF-7 Dissolving Solution

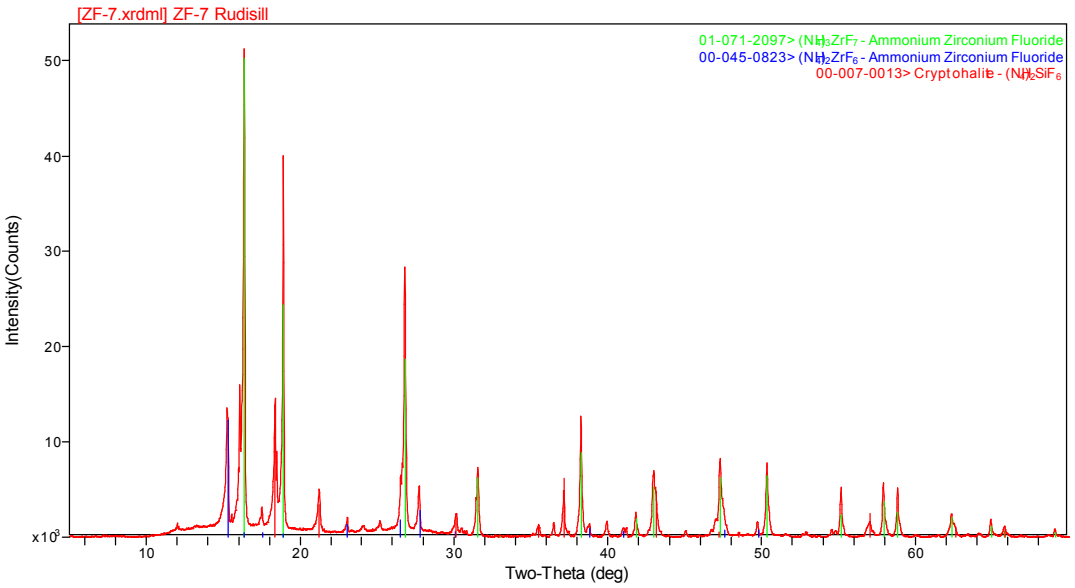

Figure 10 Zircaloy Coupons Following HF Dissolution

Experiment HF-1
[HF] = 5.0 M
60 °C, 0.33 min

Experiment HF-3
[HF] = 2.5 M
60 °C, 1.33 min

Figure 11 Dissolution Rates of Zircaloy-4 Coupons in HF

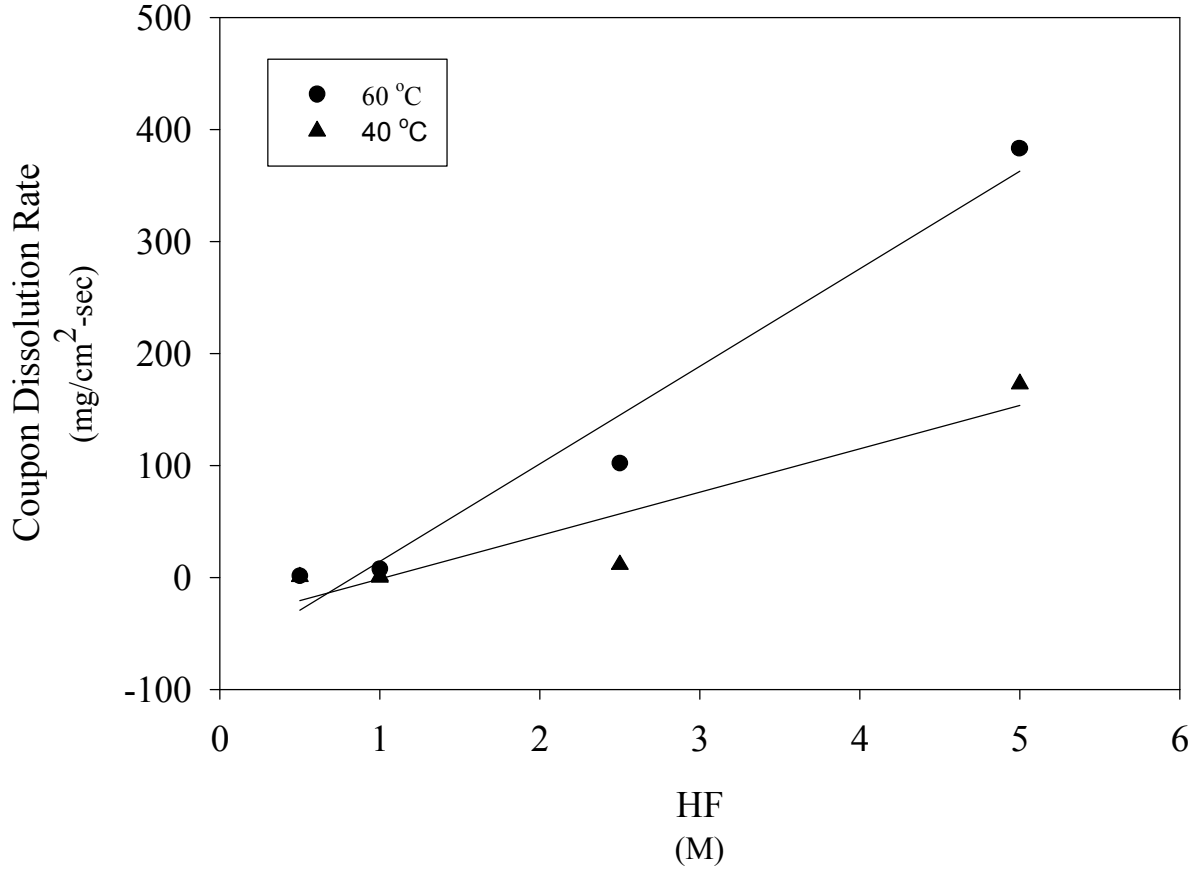

Figure 12 Oxide Layer on Zircaloy-4 Coupon Before and After Experiment HF-6

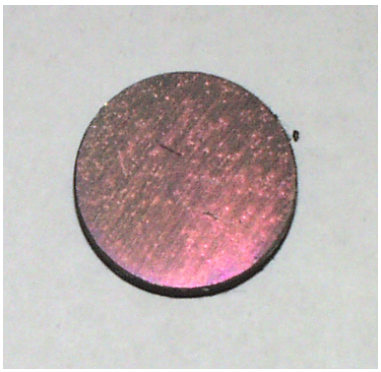

Zircaloy-4 Coupon Following 6 min in 1.0 M HF at 40 °C

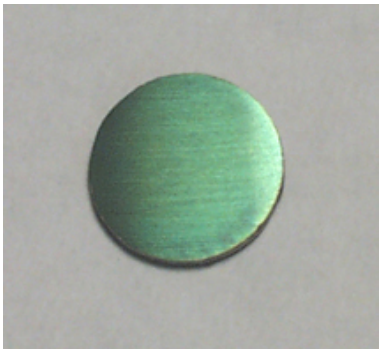

Oxidized Zircaloy-4 Coupon

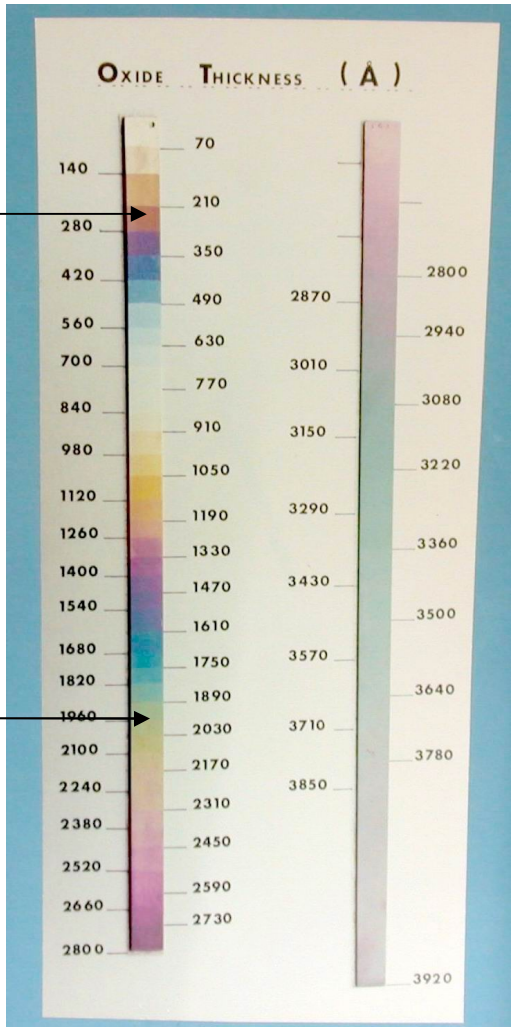

[9] Courtesy of Chalk River Laboratories, Chalk River, Ontario, Canada

Appendix A Calculation of ZIRFLEX Dissolution Rates

Effective dissolution rates were estimated for experiments ZF-4 through ZF-7 from the change in the mass to surface area ratio at the beginning and end of the dissolutions. The data (including the dissolution time, initial and final coupon mass, initial and final coupon diameter, and initial and final coupon thickness) used to calculate the rates are given in Table A.1 for each experiment.

Table A.1 Experimental Data Used to Calculate ZIRFLEX Dissolution Rates

Exp't No.	Dissol'n Time (min)	Initial Coupon Mass (g)	Initial Coupon Diameter (cm)	Initial Coupon Thickness (cm)	Final Coupon Mass (g)	Final Coupon Diameter (cm)	Final Coupon Thickness (cm)
ZF-4	12	6.6279	1.90	0.35	5.2768	1.85	0.30
ZF-5	60	6.6751	1.90	0.35	5.5643	1.86	0.31
ZF-6	60	6.5952	1.89	0.35	4.4964	1.82	0.27
ZF-7	18	6.6064	1.89	0.35	4.4996	1.81	0.27

The initial and final mass to surface area ratios were calculated from the data in Table A.1 for each coupon. The effective dissolution rates were then estimated from the change in the ratio with respect to time. The mass to surface area ratios and effective dissolution rates are given in Table A.2.

Table A.2 Calculation of Effective ZIRFLEX Dissolution Rates

Exp't No.	Initial Mass to Surface Area Ratio (mg/cm^2)	Final Mass to Surface Area Ratio (mg/cm^2)	Effective Dissolution Rate (mg/cm^2-min)
ZF-4	854	741	9
ZF-5	860	768	2
ZF-6	858	666	3
ZF-7	859	673	10

Appendix B Calculation of HF Dissolution Rates

Effective dissolution rates were estimated for the experiments performed with HF from the change in the mass to surface area ratio at the beginning and end of the dissolutions. The data (including the dissolution time, initial and final coupon mass, initial and final coupon diameter, and initial and final coupon thickness) used to calculate the rates are given in Table B.1 for each experiment.

Table B.1 Experimental Data Used to Calculate HF Dissolution Rates

Exp't No.	Dissol'n Time (min)	Initial Coupon Mass (g)	Initial Coupon Diameter (cm)	Initial Coupon Thickness (cm)	Final Coupon Mass (g)	Final Coupon Diameter (cm)	Final Coupon Thickness (cm)
HF-1	0.33	4.2538	(1)	(1)	3.3770	1.90	0.20
HF-2	0.5	4.5561	(1)	(1)	3.9189	1.95	0.23
HF-3	1.33	1.9430	(1)	(1)	0.9746	2.03	0.10
HF-4	4	1.1464	1.90	0.08	0.8080	1.85	0.07
HF-5	6	6.3801	1.91	0.36	5.8289	1.89	0.34
HF-6	6	6.3006	1.92	0.34	6.1691	1.91	0.34
HF-7	14	3.6145	1.94	0.20	3.5661	1.94	0.20
HF-8	6	5.7831	1.91	0.31	5.6721	1.90	0.31
HF-9	18	2.6089	2.00	0.12	2.4901	1.99	0.12

(1) Measurement not performed.

The initial and final mass to surface area ratios were calculated from the data in Table B.1 for each coupon. For the experiments in which the initial surface area (i.e., diameter and thickness of the coupon) was not measured, the final area was used to calculate both the initial and final mass to surface area ratios. The effective dissolution rates were then estimated from the change in the ratio with respect to time. The mass to surface area ratios and effective dissolution rates are given in Table B.2.

Exp't No.	Initial Mass to Surface Area Ratio (mg/cm^2)	Final Mass to Surface Area Ratio (mg/cm^2)	Effective Dissolution Rate (mg/cm^2-min)
HF-1	620	492	380
HF-2	617	531	170
HF-3	273	137	100
HF-4	186	140	12
HF-5	809	764	7.4
HF-6	804	794	1.6
HF-7	507	500	0.48
HF-8	762	754	1.3
HF-9	371	357	0.75